


 Cite this: *RSC Adv.*, 2021, 11, 5601

# Biohydrogen production from traditional Chinese medicine wastewater in anaerobic packed bed reactor system

 Caiyu Sun, Tao Sheng, \* Lixin Li and Lisha Yang

Three anaerobic packed bed reactors (APBR) packed with activated carbon, maifanite and tourmaline as support material were continuously operated for 165 days to generate hydrogen from traditional Chinese medicine wastewater at different organic loading rates (OLR) from 15.2 to 91.3 g COD L<sup>-1</sup> d<sup>-1</sup> by changes of hydraulic retention time (HRT) varying from 24 to 6 h. The best performance with hydrogen production rate (HPR) of 7.92 ± 0.27 mmol L<sup>-1</sup> h<sup>-1</sup> and hydrogen yield (HY) of 3.50 ± 0.09 mmol g<sup>-1</sup> COD was achieved for the reactor with tourmaline at OLR of 60.8 g COD L<sup>-1</sup> d<sup>-1</sup> (HRT = 6 h), followed by activated carbon and maifanite. The main metabolic products for each reactor were found to be acetate and butyrate in the effluent with pH range of 5.6–6.4 and microbial analysis revealed that the dominant communities in all cultures were *C. carboxidivoran* and *C. butyricum*, responsible for acetate and butyrate production respectively.

Received 1st November 2020

Accepted 20th January 2021

DOI: 10.1039/d0ra09290h

[rsc.li/rsc-advances](https://rsc.li/rsc-advances)

## Introduction

With the gradually increasing demand for clean energy, hydrogen has been envisaged as a clean energy carrier which generates only water as a product when combusted and has received increasing attention from researchers when facing the problems of environmental pollution and fossil fuel depletion in recent years.<sup>1</sup> Among the various methods for continuous hydrogen production, anaerobic fermentation is a promising technology, where microorganisms degrade biodegradable matter by hydrolysis and acidogenesis to hydrogen and soluble metabolites under conditions of oxygen absence. Anaerobic fermentation for hydrogen production can take place at ambient temperature and pressure with harmless by-products production, while enabling higher conversion efficiency and a wider range of substrate utilization when compared to other technologies.<sup>2,3</sup> The use of inexpensive substrates (*e.g.* wastewater and solid wastes) for hydrogen production is particularly attractive from an economic point of view. In China, herbal medicines are widely used by about 85% of the population, especially in Yunnan and Guangxi Province.<sup>3</sup> The traditional Chinese medicine wastewater (TCMW), produced from raw material washing, drug extraction and equipment cleaning in herbal medicine-making enterprise, comprise of the complex compounds including carbohydrates, organic acids, glycosides, anthraquinones, lignin, alkaloids, protein, starch and their hydrolysates.<sup>4</sup> The TCMW is strongly characterized by high concentration of chemical oxygen demand (COD) and

biochemical oxygen demand (BOD) in the range of 9500–18 200 mg L<sup>-1</sup> and 5500–12 200 mg L<sup>-1</sup> respectively and has the potential for hydrogen production in anaerobic fermentation system.

For anaerobic reactors for hydrogen production, continuous stirred tank reactor (CSTR), upflow anaerobic sludge bed reactor (UASB) and expanded granular sludge bed reactor (EGSB) are the widely used reactor configurations.<sup>5,6</sup> In contrast, the anaerobic packed bed reactor (APBR) receive the relative few attention compared to CSTR, UASB and EGSB. The APBR has a great advantage over the abovementioned reactors due to its simple configuration, lower construction and operation costs, because neither mechanical agitation nor external sedimentation are needed. So far, synthetic wastewaters based on glucose, sucrose or lactose have been used frequently in APBRs for process assessment, *i.e.*, determining hydrogen potential at different operational conditions. For instance,<sup>7</sup> operated two APBRs containing two different support materials to biohydrogen production from synthetic wastewater containing glucose (4000 mg L<sup>-1</sup>) and reported the highest hydrogen yield (HY) of 1.90 and 2.59 mmol mmol<sup>-1</sup> for polystyrene and expanded clay respectively at HRT = 2 h. For an APBR packed with activated carbon as support material, the glucose with concentration of 10 000 mg L<sup>-1</sup> was used as substrate, obtaining the maximum HY of 1.19 mmol mmol<sup>-1</sup> at HRT of 1 h. However, considering practical applications in wastewater treatment, the assessment of long-term operation performance and stability of APBR to treat real wastewater containing high content of carbohydrates instead of synthetic wastewater for hydrogen evolution is recommended.

College of Environmental and Chemical Engineering, Heilongjiang University of Science and Technology, Harbin 150022, China. E-mail: tsheng@usth.edu.cn



So far, the support materials, *e.g.*, activated carbon, calcium alginate, zeolite, diatomite have been successfully used to promote the granular sludge formation for the treatment of brewery wastewater, petroleum wastewater, municipal wastewater and so on.<sup>7,8</sup> Maifanite and tourmaline are promising support material due to its availability and low cost. With porous structure and large surface area, they have been widely used for heavy metal removal and dyes degradation in wastewater.<sup>9,10</sup> However, scarce studies have been carried out to report the feasibility and performance of continuous hydrogen production from wastewater using anaerobic sludge system.

In this context, the present study investigates hydrogen production performance from the TCMW containing complex compounds in three APBR systems using activated carbon, maifanite and tourmaline as support materials for long-term operation. The influence of OLR on the performance of APBR treating the TCMW and attachment/detachment process of biofilm on support material are also investigated.

## Material and methods

### Substrate

The TCMW used in this study for hydrogen production was derived from Harbin Pharmaceutical Group Co., Ltd. (Harbin, China). Table 1 reveals the main chemical characteristics of the TCMW. From Table 1, the TCMW contained a high concentration of organic matter, whereas the concentration of nitrogen and phosphorus nutrition was insufficient for anaerobic fermentation according to.<sup>12</sup> Therefore, the COD : N : P ratio of the influent was adjusted to be the level of 500 : 5 : 1 by adding a certain amount of chemicals ( $\text{NH}_4\text{Cl}$  and  $\text{KH}_2\text{PO}_4$ ) to overcome nutrient limitations. Prior to use, the TCMW was filtrated using 1 mm stainless mesh to prevent bed clog of the reactor.

### Inoculum

The microbial inoculum used for the startup of reactors was the raw sludge collected from dewatering room derived from biochemical tank in Wenchang Municipal Sewage Treatment Plant (Harbin, China) with a processing capacity of  $105 \text{ m}^3 \text{ d}^{-1}$ . The raw sludge was sieved using a stainless steel colander with a diameter of 0.5 mm to remove large particles. Referring to the method adapted by,<sup>13</sup> the aeration pretreatment endured over a total of 30 days using sucrose as carbon source with the COD

concentration of  $2 \text{ g L}^{-1}$  in sequential batch reactor (SBR), to suppress the metabolic activities of hydrogen-consuming bacteria, especially the methanogenic microorganisms. After 30 days enrichment, the sludge was used as inoculum.

### Support material

Three types of support materials packed in APBR systems for biohydrogen production were activated carbon, maifanite and tourmaline, purchased from Fidelity Water Purification Material Co., Ltd (Gongyi, China), Wunfeng Calcium Co., Ltd (Changxing, China) and Yunhai Water Purification Material Co., Ltd (Zibo, China), respectively. Their characteristics are presented in Table 2.

### Reactor setup

Three identical reactors employed in this study for continuous hydrogen production were packed with activated carbon (R1), maifanite (R2) and tourmaline (R3) respectively and were composed of reinforced fiberglass with height of 1.0 m and internal diameter of 20 cm, yielding a working volume of 30 L after packing the support material. A gas–solid–liquid separator was installed upside the reactor to prevent the sludge loss and promote the biogas release. The temperature was maintained at  $37 \pm 1 \text{ }^\circ\text{C}$  by electric jacket and a temperature sensor was placed in the reactor for real-time detection. A pH sensor was also inserted into the reactor to monitor system pH during anaerobic fermentation. An outlet was provided at the top of the reactor through which the generated biogas was collected by a water displacement method.

### Experimental design

The reactors were started up by continuous-flow mode at the increasing OLR by decreasing influent COD concentration with constant HRT of 24 h, using diluted TCMW as substrate. After successful startup, the OLR was gradually increased from 15.2 to 22.8, 36.5, 60.8, and  $91.3 \text{ g COD L}^{-1} \text{ d}^{-1}$  by decreasing HRTs from 24 h and 4 h at constant COD concentration of  $15.21 \text{ g L}^{-1}$  once a steady state was obtained at each OLR. The influent flow rate was controlled by the peristaltic pump (Model BT300, Changzhou Baist Co., Ltd., Changzhou, China) to achieve the required OLR. In this study, the steady state is defined as the state that the standard deviation of biogas production, *i.e.* hydrogen production rate (HPR) was less than 10%. The OLR schedule by changes COD concentration and HRT throughout the experiment is highlighted in Table 3.

### Analytical methods

The biogas originated from the reactors was collected and monitored by a wet gas flow meter (Model LML-3, Kesion electronics Co. Ltd., Qingdao, China). The composition of biogas, *e.g.*, hydrogen, carbon dioxide and methane, was analyzed by a gas chromatography (Model GC-2010 plus, Shimadzu, China) with nitrogen as the carrier gas at a flow rate of  $50 \text{ mL min}^{-1}$ . The gas chromatography is equipped with the hydrogen flame ionization detector (FID), thermal conductivity detector (TCD)

Table 1 Characteristics of the TCMW used in this study

Parameters	Unit	Mean values
Chemical oxygen demand (COD)	$\text{g L}^{-1}$	$15.21 \pm 0.11$
Biological oxygen demand (BOD)	$\text{g L}^{-1}$	$11.35 \pm 0.23$
Total suspended solid (TSS)	$\text{g L}^{-1}$	$0.56 \pm 0.10$
Volatile suspended solid (VSS)	$\text{g L}^{-1}$	$0.41 \pm 0.06$
Total nitrogen (TN)	$\text{g L}^{-1}$	$0.07 \pm 0.01$
Total phosphorus (TP)	$\text{g L}^{-1}$	$0.02 \pm 0.01$
pH	—	$6.62 \pm 0.28$
Alkalinity	$\text{g L}^{-1}$	$0.93 \pm 0.05$

Table 2 Characteristics of the support material used in this study

Parameters	Activated carbon	Maifanite	Tourmaline
Shape	Cylinders	Granules	Granules
Length (mm)	4.2	5.5	4.6
Diameter (mm)	3.5	3.2	3.6
Specific surface area (cm <sup>2</sup> g <sup>-1</sup> )	5.1	4.2	5.5
Point of zero charge	8.1	6.8	7.8
Roughness	15.4	14.8	17.9

Table 3 COD concentration, HRT and resulting OLR in this experiment

Stage	OLR (g COD L <sup>-1</sup> d <sup>-1</sup> )	COD concentration (g L <sup>-1</sup> )	HRT (h)
I	3.0	3.0	24
	6.0	6.0	24
	9.0	9.0	24
	12.0	12.0	24
	15.2	15.2	24
II	22.8	15.2	16
III	36.5	15.2	10
IV	60.8	15.2	6
V	91.3	15.2	4
VI	60.8	15.2	6

and flame photometric detector (FPD). The temperatures of the injection port, oven and detector were set to be 220 °C, 150 °C and 220 °C, respectively.

The composition and concentration of soluble metabolic products, *e.g.*, ethanol, acetate, butyrate, lactic acid and propionate, are analyzed by a liquid chromatography (Model LC-16P, Shimadzu, China) with a flame ionization detector (FID). In addition, a 2 m stainless steel column packed with the 70–80 meshes supporter was also equipped. The temperatures of the injection port, oven, and detector were 240 °C, 190 °C, and 240 °C, respectively. Nitrogen was used as the carrier gas at a flow rate of 30 mL min<sup>-1</sup>.

TSS and VSS (to represent microbial biomass concentration) were measured in accordance with ISO 15705:2002–11 and SIST EN 14346:2007 standardized procedures; respectively.

The analysis of COD, BOD, pH, TSS, VSS, TN, TP and alkalinity were made in accordance with Standard Methods (APHA, 2005). The sampling and analysis of bacterial communities was performed using DNA extraction, polymerase chain reaction (PCR) and pyrosequencing, referred to the study conducted by us.<sup>14</sup> Biomass adhesion to the activated carbon, maifanite and tourmaline was determined according to the methods of ref. 11.

Microbial biomass on the examined supports has been mechanically pretreated in order to release microbial biofilm in the suspension. Samples were added to 2 mL tubes with sterile zirconium beads of various sizes (0.3 g with diameter of 0.1 mm and 0.1 g with diameter of 0.5 mm; Roth). Samples were then immersed into TE buffer and homogenized (3–4 min) on a shaker (Vortex Genie2) equipped with the microcentrifuge

tube adapter (Mobio Laboratories; Carlsbad; USA). After shaking, 200 µL of suspension was used for DNA isolation. Microbial DNA was extracted and purified using Power Soil DNA Isolation Kit (Mobio Laboratories; Carlsbad; USA). The quantity of the extracted DNA was checked by measuring its absorbance on NanoVue-Plus spectrophotometer (GE Healthcare; UK).

## Results and discussion

### Hydrogen production

The temporal variation of hydrogen production rate (HPR) and hydrogen yield (HY) calculated per gram of removed COD for the tested reactors packed with activated carbon, maifanite and tourmaline at different OLRs obtained by the changes of COD concentration and HRT is depicted in Fig. 1a and b, respectively. As one can see in Fig. 1a, the three reactors showed the similar variation trend for the HPR and HY with increasing OLRs. Hydrogen started to generate on day 6, day 8 and day 6 for R1, R2 and R3, respectively, which can be attributed to the growth time of biofilm on the surface of support material.

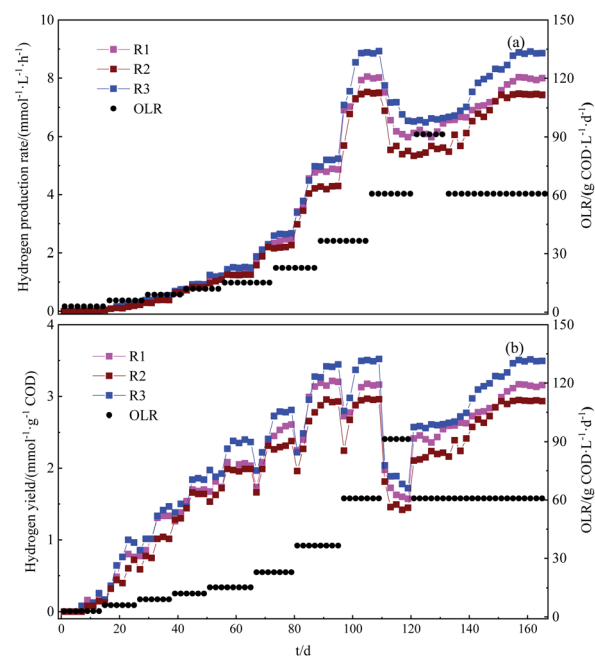


Fig. 1 Hydrogen production rate (a) and hydrogen yield (b) obtained by APBR systems with different support materials throughout the experiment.

During the start-up (stage I), the strategy of increased OLR till up to  $15.2 \text{ g COD L}^{-1} \text{ d}^{-1}$  with raised COD concentration applied to the reactor was adopted. It was found out that the HPR and HY significantly increased with the increase in OLR from  $3.0$  to  $15.2 \text{ g COD L}^{-1} \text{ d}^{-1}$  by changing influent COD from  $3000 \text{ mg L}^{-1}$  to  $15\ 210 \text{ mg L}^{-1}$ , maintaining the HRT at  $24 \text{ h}$ . The successful start-up of three reactors at the condition of OLR  $15.2 \text{ g COD L}^{-1} \text{ d}^{-1}$  gave the HPR of  $1.29 \pm 0.12 \text{ mmol L}^{-1} \text{ h}^{-1}$  in R1,  $1.15 \pm 0.15 \text{ mmol L}^{-1} \text{ h}^{-1}$  in R2 and  $1.51 \pm 0.07 \text{ mmol L}^{-1} \text{ h}^{-1}$  in R3. The HY was found to be  $2.03 \pm 0.05$ ,  $1.98 \pm 0.11$  and  $2.37 \pm 0.14 \text{ mmol g}^{-1} \text{ COD}$  for R1, R2 and R3 respectively. The increased OLR is suggested to contribute to higher hydrogen production, as more substrate will be supplied to the hydrogenic bacteria attached on support material.

During stage II, III and IV, the HRT was decreased from  $24$  to  $16$ ,  $10$  and  $6 \text{ h}$ , leading to an OLR of  $22.8$ ,  $36.5$  and  $60.8 \text{ g COD L}^{-1} \text{ d}^{-1}$ , respectively. The HPR increased to the highest level of  $7.33 \pm 0.21$ ,  $6.40 \pm 0.12$  and  $7.92 \pm 0.27 \text{ mmol L}^{-1} \text{ h}^{-1}$  for R1, R2 and R3 respectively, at OLR of  $60.8 \text{ g COD L}^{-1} \text{ d}^{-1}$ . The higher HPR observed by applying increasing OLR to the reactors was a consequence of the increasing availability of organic matter. For HY, these values raised up to  $3.19 \pm 0.06$ ,  $2.93 \pm 0.08$  and  $3.433 \pm 0.11 \text{ mmol g}^{-1} \text{ COD}$  for R1, R2 and R3 respectively as OLR increased to  $36.5 \text{ g COD L}^{-1} \text{ d}^{-1}$ . However, instant increase was not observed with higher OLR of  $60.8 \text{ g COD L}^{-1} \text{ d}^{-1}$ .

At stage V, the OLR was further increased to  $91.3 \text{ g COD L}^{-1} \text{ d}^{-1}$ , corresponding to the HRT of  $4 \text{ h}$ . This was accompanied with the obvious decrease in HPR and HY to  $6.08 \pm 0.13 \text{ mmol L}^{-1} \text{ h}^{-1}$  and  $1.60 \pm 0.05 \text{ mmol g}^{-1} \text{ COD}$  respectively in R1. Similarly, in R2 the HPR and HY was decreased to  $5.52 \pm 0.32 \text{ mmol L}^{-1} \text{ h}^{-1}$  and  $1.45 \pm 0.09 \text{ mmol g}^{-1} \text{ COD}$ , respectively. On the other hand, in R3 exhibited the highest hydrogen production performance, the decline in HPR and HY was found to be the level of  $6.82 \pm 0.25 \text{ mmol L}^{-1} \text{ h}^{-1}$  and  $1.79 \pm 0.04 \text{ mmol g}^{-1} \text{ COD}$  respectively, though more organic matter would be supplied to the system. Similar phenomenon was also reported by Xu *et al.* (2019), who assessed the HPR and HY performance from glucose-based wastewater in APBR system filled with activated carbon with increasing OLR. They observed that the increased HPR from  $0.79 \pm 0.02$  to  $12.25 \pm 0.08 \text{ mmol L}^{-1} \text{ h}^{-1}$  and HY from  $1.48 \pm 0.02$  to  $3.41 \pm 0.16 \text{ mmol g}^{-1} \text{ COD}$  was associated with the increment of OLR from  $11.5$  to  $86.1 \text{ g COD L}^{-1} \text{ d}^{-1}$ , but higher OLR of  $100.3 \text{ g COD L}^{-1} \text{ d}^{-1}$  provoked an fast reduction of HPR and HY to  $0.34 \pm 0.03 \text{ mmol L}^{-1} \text{ h}^{-1}$  and  $0.16 \pm 0.03 \text{ mmol g}^{-1} \text{ COD}$ , respectively.

Afterwards, the HRT was adjusted to  $6 \text{ h}$  again, equivalent to OLR of  $60.8 \text{ g COD L}^{-1} \text{ d}^{-1}$ , at stage VI in order to prevent the failure of the reactors. After about  $45$  days operation, the reactors can be restored entirely with increasing HPR and HY. The final HPR was determined to be  $7.97 \pm 0.33$ ,  $7.45 \pm 0.17 \text{ mmol L}^{-1} \text{ h}^{-1}$  and  $8.85 \pm 0.22 \text{ mmol L}^{-1} \text{ h}^{-1}$  for R1, R2 and R3 respectively, while HY was  $3.11 \pm 0.14$ ,  $2.93 \pm 0.07$  and  $3.44 \pm 0.12 \text{ mmol g}^{-1} \text{ COD}$ . These values were almost equivalent to that obtained at OLR of  $60.8 \text{ g COD L}^{-1} \text{ d}^{-1}$ . All in all, although there was on difference between the HY for OLR of  $36.5$  and  $60.8 \text{ g COD L}^{-1} \text{ d}^{-1}$ , taking into account the HPR and construction cost, the OLR of  $60.8 \text{ g COD L}^{-1} \text{ d}^{-1}$  corresponding

to HRT of  $6 \text{ h}$  was considered as the optimum operational condition for hydrogen production in each APBR.

In APBR, the support material plays an important role in the adhesion and immobilization of bacterial biofilm and their characteristics can strongly affect the performance of hydrogen production of the reactor at designed operation condition. Therefore, the different support material examined in this study exhibited an obvious influence on the HPR and HY at OLR between  $15.2 \text{ g COD L}^{-1} \text{ d}^{-1}$  and  $91.3 \text{ g COD L}^{-1} \text{ d}^{-1}$ , as illustrated in Fig. 1b. The highest value of HPR and HY was observed in the reactor filled with tourmaline (R3), followed by the reactors packed with activated carbon (R1) and maifanite (R2) at the same OLR condition. The results obtained indicated that the performance of APBRs could be strongly influenced by characteristics of support materials. Surface hydrophobicity has been described as one of the most important factors involved in bacterial adhesion process.<sup>13</sup> The results of contact angle measurements revealed that  $\theta$  value for tourmaline was  $105^\circ$ , while high porosity of maifanite and activated carbon (*i.e.* materials predominantly containing micro- and mesopores) prevented formation of water droplets and subsequent  $\theta$  measurements. Therefore, the results of this analysis have shown that tourmaline carriers were hydrophobic, while maifanite and activated carbon were found to be hydrophilic. In regard to cell affinity for different support materials, hydrophobicity index of inoculum was measured. Its value of  $75.6$  showed hydrophobic nature of present microbial cells in the inoculum, suggesting higher adhesion of bacteria on tourmaline, as this material was shown to be hydrophobic. In addition, tourmaline, as support material of the APBR, could enable higher performance in terms of hydrogen production than activated carbon and maifanite, which is closely related to the numerous macropores on the surface of tourmaline, resulting in large specific surface area, since these pores can contribute to adhesion and immobilization of microorganisms on the surface.<sup>15,16</sup>

Therefore, the highest HPR of  $7.92 \pm 0.27 \text{ mmol L}^{-1} \text{ h}^{-1}$  and HY of  $3.5 \pm 0.08 \text{ mmol g}^{-1} \text{ COD}$  was obtained in the APBR system packed with tourmaline at OLR of  $60.8 \text{ g COD L}^{-1} \text{ d}^{-1}$ , corresponding to HRT  $6 \text{ h}$ . For comparison, operating the APBR with Mutag BioChip™ as support material to treat glucose-based wastewater for biohydrogen production, the highest HPR and HY reached was  $16.65 \text{ mmol L}^{-1} \text{ h}^{-1}$  and  $1.80 \text{ mmol mmol}^{-1} \text{ glucose}$  respectively at OLR of  $72.0 \text{ g COD L}^{-1} \text{ d}^{-1}$  in the study conducted.<sup>17</sup> The result obtained in this study is lower in comparison to the abovementioned studies, because the TCMW with complex compounds is hard to be utilized by anaerobic microorganisms when compared to glucose or sucrose.

Regarding hydrogen content present in the biogas produced from three reactors, the OLR and support materials exhibited no influence on hydrogen content and biogas composition. The main composition of biogas were hydrogen, nitrogen and carbon dioxide without the existence of methane, which indicated that the methanogenic activities were completely suppressed. The hydrogen content in all the cases was detected to be in the range of from  $54.3\%$  to  $58.4\%$  (data not shown).

## Soluble metabolic products

The production of soluble metabolic products, *i.e.*, volatile fatty acids and alcohols can take place during anaerobic fermentation of organic matter, along with hydrogen, carbon dioxide and other byproducts.<sup>18</sup> The analysis and distribution of final metabolic products during anaerobic fermentation in the reactors with different support materials for every OLR tested is presented in Fig. 2. After successful start-up, the observed main metabolic products in the effluent of all the reactors at different OLRs from 15.2 and 91.3 g COD L<sup>-1</sup> d<sup>-1</sup> were acetate and butyrate accompanied with a small amount of ethanol, indicating the dominant pathway of hydrogen production were acetate-type (eqn (1)) and butyrate-type fermentation (eqn (2)). In addition, the concentration of propionate and lactose which have proven to lower hydrogen production were in low level of <45 mg L<sup>-1</sup> in this study, suggesting the cultures were metabolically appropriate for hydrogen production.



The concentration of acetate and butyrate in R3 system was highest, followed by R1 and R2, at same OLR condition. This was in accordance with superior hydrogen production performance exhibited by R3. The increasing OLR expect for 91.3 g COD L<sup>-1</sup> d<sup>-1</sup> can improve the production of acetate and butyrate, consequently resulting in the increase in HPR. The acetate and butyrate concentration was in the range of 456.8–766.4 mg L<sup>-1</sup> and 388.9–566.2 mg L<sup>-1</sup>, respectively, in R1. Similarly, the detected concentration of acetate and butyrate were within the range of 400.7–698.4 mg L<sup>-1</sup> and 328.9–508.9 mg L<sup>-1</sup> respectively in R1 while the same were found to be 512.3–893.2 mg L<sup>-1</sup> and 412.7–600.8 mg L<sup>-1</sup> respectively in R2. The pH values in all the cultures were measured to be in the range of 5.6–6.4, which is typical for acetate and butyrate fermentation.<sup>19,20</sup>

The ratio of acetate/butyrate has been considered as a crucial factor for evaluating hydrogen production efficiency in anaerobic fermentation system.<sup>17</sup> Usually, the higher hydrogen

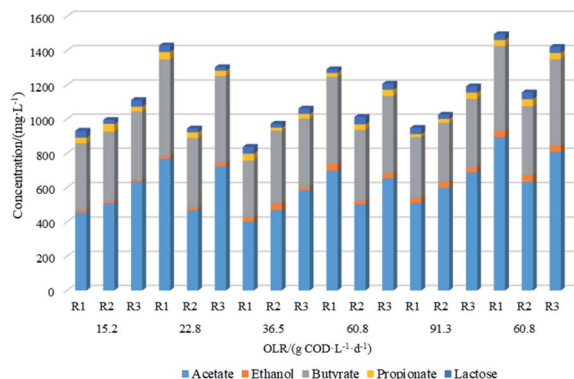


Fig. 2 Variation of soluble metabolic products exhibited by APBR systems at various OLRs.

production efficiency correlated with the higher acetate/butyrate ratio. Acetate/butyrate ratios for the APBR systems examined were calculated as per the values taken from Fig. 2. When the OLR of R3 increased from 15.2 and 60.8 g COD L<sup>-1</sup> d<sup>-1</sup>, the acetate/butyrate ratio raised from 1.45 to 1.81. However, when OLR increased to 91.3 g COD L<sup>-1</sup> d<sup>-1</sup>, the ratio diminished to 1.62. Similar behaviour was observed in R1 and R2 with ratio range of 1.17–1.48 and 1.11–1.44 respectively, corresponding to the lower hydrogen production compared to R3. This phenomenon was also observed in other studies using other anaerobic reactors for hydrogen production, conducted by,<sup>21</sup> who observed the highest HY of 12.51 mmol mmol<sup>-1</sup> at the maximum acetate/butyrate ratio of 1.3 in continuous mixed immobilized sludge reactor.

## Biofilm attachment

It is generally believed that the immobilization of biofilm developed on the surface of support material in APBRs goes through the process of attachment, growth and detachment, of which the net result strongly influences the performance of the reactors.<sup>22</sup> Fig. 3a reveals the biomass amount attached on support material in the reactors investigated in this study as a function of OLR. From Fig. 3a, it can be found clearly that the biomass amount increased from 0.048 to 0.095 g VSS g<sup>-1</sup> support for activated carbon (R1), from 0.049 to 0.083 g VSS g<sup>-1</sup> support for maifanite (R2) and from 0.058 to 0.1 g VSS g<sup>-1</sup> support for tourmaline (R3) when the OLR increased from 15.2 g COD L<sup>-1</sup> d<sup>-1</sup> to 60.8 g COD L<sup>-1</sup> d<sup>-1</sup>. This behavior was in accordance with the results of,<sup>23</sup> who observed the increased biomass amount with ascended OLR in the APBR systems with expanded clay and polystyrene as support material. This can be

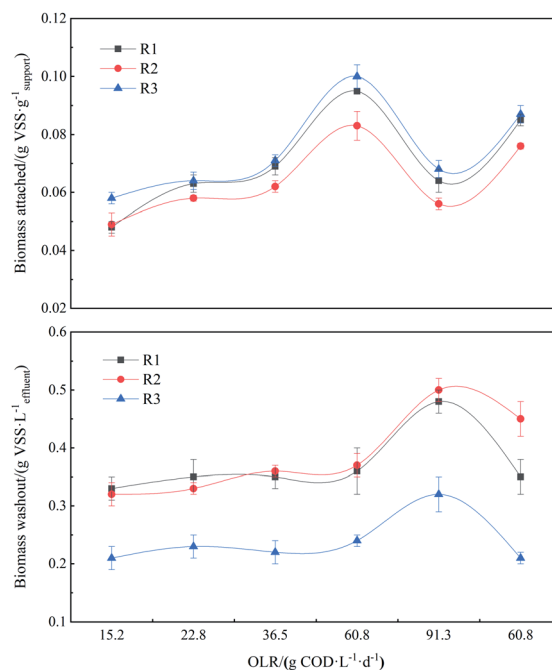


Fig. 3 The profile of biomass attachment (a) and biomass washout (b) for each reactor at different OLRs.

attributed to the fundamental that the accumulation of biofilm is higher at a higher substrate loading rate in certain range, as the availability of carbohydrates affects significantly the extracellular polymeric substances (EPS) synthesized inside and outside the biofilm, subsequently influencing biofilm growth and structures.<sup>23</sup> As is known to all, EPSs such as polysaccharides are key compounds for microbial adhesion. The presence of improved carbohydrates may favor EPSs production and subsequently the biomass amount. At the same OLR condition, tourmaline (R3) with larger surface gave the higher biofilm amount attached than activated carbon (R1) and maifanite (R2), which is suggested to contribute the superior performance of hydrogen production in R1 system, because a greater quantity of hydrogen-producing bacteria may attach on tourmaline relative to activated carbon and maifanite. As the OLR increased to  $91.3 \text{ g COD L}^{-1} \text{ d}^{-1}$ , these values of biomass amount dropped to 0.064, 0.056 and  $0.068 \text{ g VSS g}^{-1}$  support for R1, R2 and R3 respectively, which may contribute to the decline in HPR and HY for each reactor.

As other studies stated, although the high OLR can increase the biofilm thickness, the weaker attachment on support material especially for short HRT accelerates the exfoliation of some biofilm from support material due to the function of due to particle–particle collisions. The data illustrated in Fig. 3b can validate the aggravation of biofilm detachment at high OLR. The effluent VSS for each reactor at OLR of  $91.3 \text{ g COD L}^{-1} \text{ d}^{-1}$  with short HRT of 4 h was higher in comparison to other stages. Moreover, concentration of effluent VSS was the highest in R2 with the lowest hydrogen production performance, followed by R1 and R3. For each reactor, effluent VSS concentration remained virtually constant as OLR increased from  $15.2 \text{ g COD L}^{-1} \text{ d}^{-1}$  to  $60.8 \text{ g COD L}^{-1} \text{ d}^{-1}$ .

At OLR of  $60.8 \text{ g COD L}^{-1} \text{ d}^{-1}$  which determined the highest hydrogen production performance in all the cases, biomass yield was calculated as the sum of biomass attached and washed in the effluent per unit of COD converted and these values were 0.16, 0.09 and  $0.14 \text{ g VSS g}^{-1} \text{ COD}$  converted for R1, R2 and R3, respectively. It was worth noting that biomass yield in R3 with higher HPR and HY was lower than that of R2, consistent with the results of ref. 20 who observed the inverse relationship between biomass yield and hydrogen production performance. It is likely that lower performance exhibited by R1 with higher biomass yield relative to R3 is the consequence of higher biomass detachment rate (Fig. 3b), resulting in shorter biomass retention.

### Microbial community structure

The analysis and distribution of microbial communities from the samples taken from the initial inoculum and the reactors at the end of operation was performed. As shown in Fig. 4, the analysis of microbial community revealed the microbial diversity in the initial inoculum was generally higher than those from the reactors after 152 days of operation. The archaeal community has much higher relative abundance compared to the immobilized biofilm adhered to the support materials of the reactors, indicating the operation conditions employed in this study encourage the selection and accumulation of non-

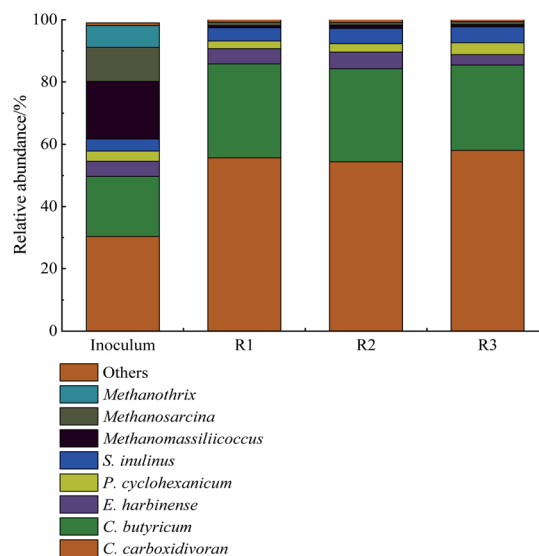
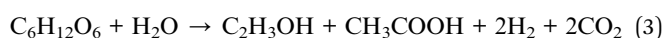


Fig. 4 Microbial communities of the initial inoculum and the reactors at the end of operation.

methanogenic archaeal communities. There was no difference with regards to the diversity of bacterial communities among the reactors examined while a slight difference in relative abundance was observed. This showed that the different support materials do not take a major influence to the bacterial structure. The bacterial communities involved in hydrogen production were founded to be comprised of *C. carboxidivoran*, *C. butyricum*, *E. harbinense*, *C. carboxidivoran* was the dominant community, followed by *C. butyricum* for each reactor. The role of member of the *C. carboxidivoran* is responsible for acetate production along with hydrogen<sup>24</sup> and the relative abundance of the same was found to be 53.7%, 52.4% and 58.1% at the end of operation for R1, R2 and R3 respectively. The presence of *C. butyricum* with relative abundance of 30.1%, 29.8% and 28.3% for R1, R2 and R3 respectively executes the conversion of substrate to butyrate, accompanied with hydrogen production. High production of hydrogen in all reactors was achieved via the metabolism of *C. carboxidivoran* and *C. butyricum*. The highest relative abundance of *C. carboxidivoran* and *C. butyricum* decided the best performance of hydrogen production presented by the APBR packed with tourmaline (Fig. 1). In other studies for anaerobic hydrogen evolution conducted by,<sup>25,26</sup> *C. carboxidivoran* and *C. butyricum* as dominant communities also played the major role in high-efficient hydrogen production.

*E. harbinense* with relative abundance of <5.5% for all the reactors was in charge of the low-concentration ethanol observed in the effluent of three APBRs (Fig. 2). A small amount of hydrogen was generated with the production of ethanol (below  $50 \text{ mg L}^{-1}$ ) according to eqn (3). Wang claimed this fermentation pathway with ethanol as the dominant metabolic product was a high-efficient route for hydrogen production at pH of below 4.0. Obviously, the cultures with pH above 5.0 were unfavorable for this fermentation pathway.<sup>13</sup>



The fermentative products of *P. cyclohexanicum* and *S. inulinus* are propionic acid and lactic acid, respectively, which are adverse to hydrogen production. Nevertheless, the low relative abundance of *P. cyclohexanicum* and *S. inulinus* was observed in the cultures, which corresponded to low amounts of propionic acid and lactic acid, indicating the existence of propionic acid and lactic acid in the effluent has negligible influence on hydrogen production. Barros *et al.* (2011) reported these species during anaerobic hydrogen production in anaerobic fixed-bed reactor.<sup>23</sup>

### Feasibility for continuous and long-term operation

The adhesion and accumulation of biofilm on support material depends greatly on many factors, including the characteristics and concentration of substrate, the velocity of the liquid phase (HRT), the concentration of particles, pH and so on. Although the TCMW used in this study contains sophisticated components, which make it, harder to be used by anaerobic microorganisms relative to synthetic wastewater based on sucrose or glucose, the continuous and long-term operation of three APBRs with different support materials over 165 days was successfully completed for hydrogen production at different OLRs. It is difficult to compare hydrogen production performance with other studies due to the different conditions adopted. To our best knowledge, only two studies have been done to investigate the hydrogen generation performance by the APBR from the real wastewater. Using sugarcane vinasse and soft-drinking wastewater as substrate,<sup>20</sup> successfully demonstrated the operation of APBRs packed with low-density polyethylene as support material for hydrogen production, achieving the HPR of  $0.40 \text{ L L}^{-1} \text{ h}^{-1}$ . In this study, the APBR filled with tourmaline exhibited the best performance with HPR of  $7.92 \pm 0.27 \text{ mmol L}^{-1} \text{ h}^{-1}$  and HY of  $3.44 \pm 0.12 \text{ mmol g}^{-1} \text{ COD}$  at optimized OLR condition by changing HRT, which highlighted the feasibility of APBR for treating the TCMW. It is difficult to compare hydrogen production performance with other studies due to the different conditions adopted. The findings observed make the use of the APBR even more feasible and promising for continuous hydrogen production from wastewater. In the future work, the methane production from hydrogen producing effluent rich in the soluble metabolic products which are easier to be catabolized by methanogenic microorganisms in the APBR will be paid more attention. Besides, more types of wastewater should be examined, and the operational strategy of the APBR can be according to the characteristics of wastewater. For instance, regarding the cassava alcohol wastewater, the APBR can consider to be operated under thermophilic condition without energy input as per its feature of high temperature (80–100 °C).

## Conclusions

This study verified the feasibility of continuous hydrogen production from the traditional Chinese medicine wastewater by anaerobic packed bed reactor at different organic loading rates. Tourmaline was the most suitable support material compared with activated carbon and maifanite, since the

highest hydrogen production rate (HPR) of  $7.92 \pm 0.27 \text{ mmol L}^{-1} \text{ h}^{-1}$  and hydrogen yield (HY) of  $3.50 \pm 0.09 \text{ mmol g}^{-1} \text{ COD}$  was achieved in the reactor packed with tourmaline at OLR of  $60.8 \text{ g COD L}^{-1} \text{ d}^{-1}$  (HRT = 6 h), which was maybe related to lower biomass detachment rate rather than higher biomass attachment rate. The analysis and distribution of microbial communities revealed clearly the variation of hydrogen production and soluble metabolic products concentration.

## Conflicts of interest

There are no conflicts to declare.

## Acknowledgements

This work was financed by grants from the project of “National Natural Science Foundation (51908200)”.

## References

- 1 P. Khongkliang, P. Kongjan, B. Utarapichat, A. Reungsang and S. Thong, *Int. J. Hydrogen Energy*, 2017, **42**, 27584–27592.
- 2 P. Mario, D. Z. Gregor, F. Lijana, L. Romana Marinšek, T. Marina and Z. Bruno, *J. Cleaner Prod.*, 2017, **166**, 519–529.
- 3 J. Li, B. Li, G. Zhu, N. Ren, L. Bo and J. He, *Int. J. Hydrogen Energy*, 2007, **32**, 3274–3283.
- 4 T. Nandy and S. Kaul, *Water Res.*, 2001, **35**, 351–362.
- 5 M. K. Arantes, H. J. Alves, R. Sequinel and D. Silva, *Int. J. Hydrogen Energy*, 2017, **42**, 26243–26256.
- 6 J. Bárcenas-Ruiz, L. Arellano-García, L. B. Celis, F. Alatríste-Mondragón and E. Flore, *Biochem. Eng. J.*, 2016, **107**, 75–84.
- 7 G. Mujtaba and K. Li, *Water Res.*, 2017, **120**, 174–184.
- 8 S. Xu, C. He, L. Luo, P. He and L. Cui, *Bioresour. Technol.*, 2015, **196**, 606–612.
- 9 C. Chen, J. Liang, B. Yoza, B. Li and Q. Wang, *Bioresour. Technol.*, 2017, **243**, 620–627.
- 10 N. Inchaurredo, J. Font and C. P. Ramos, *Appl. Catal., B*, 2016, **181**, 481–494.
- 11 A. R. Barros, E. Amorim, C. M. Reis, G. M. Shida and E. L. Silval, *Int. J. Hydrogen Energy*, 2010, **35**, 3379–3388.
- 12 D. Ochs, W. Wukovits and W. Ahrer, *J. Cleaner Prod.*, 2010, **18**, S88–S94.
- 13 B. Wang, Y. Li and N. Ren, *Int. J. Hydrogen Energy*, 2013, **38**, 4361–4367.
- 14 C. Sun, F. Liu, Z. Song, J. Wang, Y. Li, Y. Pan, T. Sheng and L. Li, *Bioresour. Technol.*, 2019, **276**, 65–73.
- 15 Z. Ma, C. Li and H. Su, *Renewable Energy*, 2017, **105**, 458–464.
- 16 V. M. Blanco, G. H. Oliveira and M. Zaiat, *Renewable Energy*, 2019, **139**, 1310–1319.
- 17 P. Muri, R. Marinek-Logar, P. Djinovi and A. Pintar, *Enzyme Microb. Technol.*, 2018, **111**, 87–96.
- 18 R. Kothari, V. Kumar, V. V. Pathak and V. V. Tyagi, *Int. J. Hydrogen Energy*, 2017, **42**, 4870–4879.
- 19 L. Ding, J. Cheng, R. Lin, C. Deng and D. J. Murphy, *J. Cleaner Prod.*, 2019, **251**, 119666.
- 20 G. Peixoto, N. K. Saavedra, M. B. A. Varesche and M. J. Zaiat, *Int. J. Hydrogen Energy*, 2011, **36**, 8953–8966.

- 21 W. Han, B. Wang, Y. Zhou, D. X. Wang, Y. Wang, L. Yue, Y. Li and N. Ren, *Bioresour. Technol.*, 2012, **110**, 219–223.
- 22 C. Lin, S. Wu and J. Chang, *Int. J. Hydrogen Energy*, 2006, **31**, 2200–2210.
- 23 A. Barros, M. Adorno, I. Sakamoto, S. Maintinguer, M. Varesche and E. Silva, *Bioresour. Technol.*, 2011, **102**, 3840–3847.
- 24 J. Leite, B. Fernandes, E. Pozzi, M. Barboza and M. Zaiat, *Int. J. Hydrogen Energy*, 2008, **33**, 579–586.
- 25 H. Argun and S. Dao, *Int. J. Hydrogen Energy*, 2017, **42**, 2569–2574.
- 26 M. Soltan, M. Elsamadony and A. Tawfik, *Appl. Energy*, 2017, **185**, 929–938.